Catalysis Today 59 (2000) 313–321

www.elsevier.com/locate/cattod

Catalytic activity of Pt and tungstophosphoric acid supported on MCM-41 for the reduction of NO_x in the presence of water vapor

A. Jentys[a,b,*], W. Schießer[a], H. Vinek[a]

[a] *Technische Universität Wien, Institut für Physikalische und Theoretische Chemie, Getreidemarkt 9/156, A-1060 Wien, Austria*

[b] *Technische Universität München, Lehrstuhl für Technische Chemie II, Lichtenbergstr. 4, 85747 Garching, Germany*

Abstract

The catalytic activity of tungstophosphoric acid and Pt loaded MCM-41 for the catalytic reduction of NO_x with propene in the presence of water vapor was studied. Pt/MCM-41 was found to be most active, the loading with $H_3PW_{12}O_{40}$ led to an improved selectivity to N_2 formation and to an enhanced activity in the presence of water vapor. Hydrated tungstophosphoric acid generated additional sorption sites for C_3H_6 and led to a higher local concentration of the reducing agent on the catalyst surface, which was found to increase the activity of the Pt and $H_3PW_{12}O_{40}$ loaded catalysts in the presence of water vapor.

Keywords: Pt/MCM-41; Tungstophosphoric acid; Catalytic activity; NO_x reduction

1. Introduction

Nitrogen oxides, formed during combustion processes in power plants, waste incinerators and diesel engines, are among the major air pollutants leading to the formation of photochemical smog and acid rain [1]. Thus, the catalytic reduction of NO_x plays an important role in the transformation of combustion processes into an environment-friendly technology [2]. At present, catalysts based on titanium- and vanadium-oxides, together with ammonia as reducing agent, are typically applied to remove nitrogen oxides from flue-gas streams of stationary sources [3]. For mobile sources, however, extensive research is currently carried out to find alternative catalytic systems in order to replace NH_3 with environmentally more acceptable reducing agents such as hydrocarbons [4]. Catalysts based on transition metal containing zeolites, e.g. Cu/ZSM5 [5] and Co/ZSM5 [6,7], were investigated in the first place, but the strong decrease in the activity when H_2O and/or SO_2 are present in the reactant [8–10] led to the development of alternative catalysts such as Fe/ZSM5 [9,11,12], Pt/ZSM5 [13] and Pt group metals supported on SiO_2 and Al_2O_3 [14,15].

In order to combine the advantages of zeolites and oxide based systems, we studied the catalytic properties of noble metals supported on mesoporous molecular sieves with MCM-41 type structure. As the acid sites of these materials were found to be only weakly acidic [16], the catalysts were additionally impregnated with tungstophosphoric acid, a procedure known to generate strong Brønsted acidic sites on MCM-41 type materials [17].

---

[*] Corresponding author.

E-mail address: jentys@tuwien.ac.at (A. Jentys)

0920-5861/00/$ – see front matter © 2000 Elsevier Science B.V. All rights reserved.
PII: S0920-5861(00)00297-2

2. Experimental

2.1. Materials

The synthesis of siliceous MCM-41 was carried out according to [18] using fumed silica (SiO_2) as Si-source, hexadecyltrimethylammonium bromide (CTABr) as template molecule and tetramethylammoniumhydroxide-pentahydrate (TMAOH) as complexing agent. The gel composition was: SiO_2:TMAOH:CTABr:H_2O=1:0.19:0.27:40. The synthesis gel was prepared by solving TMAOH and CTABr in distilled water under stirring and after a clear solution was obtained, SiO_2 was added. After an initial aging at room temperature for 24 h, the condensation of the solid was carried out at 423 K for 48 h in a Teflon autoclave. The product was filtered, washed with distilled water and dried in air at 323 K. The template removal was carried out by calcination in synthetic air at 813 K for 10 h using a heating rate of 1 K min^{-1}.

The mesoporous support was impregnated with an aqueous solution of $PtCl_4$ [9], of $H_3PW_{12}O_{40}$ [17] and of $PtCl_4$ and $H_3PW_{12}O_{40}$ [20]. The Pt loading of the catalysts was 1.6 wt.%, the $H_3PW_{12}O_{40}$ loading was varied between 0 and 60 wt.%. In this paper, the catalysts are denoted as Pt/MCM-41, HPW(*X*)/MCM-41 and Pt/HPW(*X*)/MCM-41 (*X* being the $H_3PW_{12}O_{40}$ loading in wt.%).

After impregnation, the catalysts were dried at 373 K overnight, calcined in synthetic air at 773 K for 3 h (heating rate 10 K min^{-1}), crushed in a mortar and sieved. A grain size smaller than 180 μm was used for the kinetic experiments.

2.2. Characterization of the structural properties

The structure of the mesoporous MCM-41 type support and of the catalysts was characterized by X-ray powder diffraction in an angular range between 1° and 40° (2θ).

The specific surface area (BET method) and pore size distribution (Kelvin equation [21,22]) of support before and after loading with Pt and $H_3PW_{12}O_{40}$ were determined from N_2 adsorption isotherms at 77 K. The BET surface area of the MCM-41 support was found to be 1006 m^2/g.

The number of accessible Pt atoms of Pt/MCM-41 was determined by H_2-chemisorption carried out in a volumetric system. Before the experiments, the catalysts were reduced at 773 K for 2 h in flowing H_2 and evacuated at 773 K for 2 h ($\sim 10^{-6}$ mbar). A H_2 sorption isotherm was measured at 295 K by exposing the catalyst to decreasing amounts of H_2. The H/Pt ratio was calculated from the hydrogen uptake obtained from an extrapolation of the horizontal part of the isotherm to zero pressure. Due to the partial reduction of $H_3PW_{12}O_{40}$ under the conditions of the H_2-chemisorption experiment, this method was found to be not suitable for determining the metal dispersion of $H_3PW_{12}O_{40}$ containing catalysts.

IR-spectroscopy was used to characterize the type and concentration of the acid sites (adsorption of pyridine) and the number of accessible Pt atoms for $H_3PW_{12}O_{40}$ containing catalysts (adsorption of CO). The samples were prepared as self-supporting wafers and investigated in transmission mode with a resolution of 4 cm^{-1} using a Bruker IFS 28 spectrometer. The catalysts were either activated in vacuum ($\sim 10^{-6}$ mbar) at 773 K for 1 h or reduced in H_2 at 773 K for 1 h (temperature increase of 10 K min^{-1} from ambient temperature). The number of accessible Pt atoms was calculated from the integral intensity of the band at 2074 cm^{-1} using Pt/MCM-41 (where the number of surface atoms was determined by H_2-chemisorption) as standard. The structural data of all catalysts investigated are summarized in Table 1.

2.3. Catalytic activity

The catalytic activity was studied in a quartz reactor (i.d. 8 mm) containing 100 mg catalyst. The temperature was measured with a thermocouple placed in direct contact to the catalyst bed. Four mass flow controllers (Brooks 5850E) were used to obtain a reactant gas mixture with the following composition: 1010 ppm NO (about 91 ppm NO was oxidized in the reaction system to NO_2), 1012 ppm C_3H_6 and 4.9 vol.% O_2. Helium was used as carrier gas. Up to 8 vol.% water vapor was added into the gas stream using a syringe pump. The total flow rate of 100 cm^3/min used resulted in a space velocity of $W/F=6\times10^{-2}$ g s cm^{-3}. Reactants and products were analyzed with a chemiluminescence NO/NO_2 analyzer and a gas chromatograph using a TCD and an FID detector. A Poraplot-Q column for the separation of CO_2, N_2O, C_3H_6 and H_2O, and an Molsieve 5 Å column for the separation of O_2,

Table 1
Composition and structural properties of the catalysts

Sample	$H_3PW_{12}O_{40}$ (wt.%)	Pt (wt.%)	H/Pt ratio (H_2-chemisorption, CO adsorption)	Accessible Pt atoms (mmol g^{-1})	Pore radius (Å)
Pt/MCM-41	–	1.61	0.63	0.052	15.5
Pt/HPW(15)/MCM-41	15	1.61	0.16	0.013	n.d.
Pt/HPW(30)/MCM-41	30	1.60	0.31	0.026	15
Pt/HPW(60)/MCM-41	60	1.64	0.10	0.008	n.d.

N_2 and CO were used. Before each reaction, the catalysts were activated in He at 773 K for 1 h. The conversion was measured in a temperature range between 453 and 773 K.

3. Results

The conversion of NO_x and C_3H_6 as function of the temperature is shown in Fig. 1. The maximum NO_x conversion and the selectivity to N_2 formation are summarized in Table 2.

The conversion of NO_x and C_3H_6 started at the same temperature and increased with increasing temperature until the total conversion of propene was reached. At this temperature, the maximum conversion of NO_x was obtained, a further temperature increase led to a decrease in the NO_x conversion, while the hydrocarbon conversion level remained at 100%. The highest NO_x conversion was observed for Pt/MCM-41 and it decreased with the $H_3PW_{12}O_{40}$ loading of the catalysts, while the selectivity to N_2 formation increased from 35 (Pt/MCM-41) up to 45% (Pt/HPW(60)/MCM-41) on the tungstophosphoric acid containing catalysts. Also the temperature where the maximum NO_x conversion was reached increased with the $H_3PW_{12}O_{40}$ loading of the catalysts.

The effect of the oxygen concentration on the NO_x conversion over Pt/MCM-41 and Pt/HPW(30)/MCM-41 at 513 K is compared in Fig. 2. At an O_2 concentration of 10 vol.%, the same level of activity was observed on both catalysts. With decreasing O_2 concentration, the NO_x conversion strongly increased on Pt/MCM-41 until a maximum conversion of 92% was reached at an O_2 concentration of 0.6 vol.%. On the contrary, on Pt/HPW(30)/MCM-41 the NO_x conversion decreased continuously with decreasing oxygen concentration in the feed. In the absence of oxygen, both catalysts did not show any NO_x conversion. The selectivity towards the formation of N_2 increased with decreasing oxygen concentration from 30 (9.8 vol.% O_2) up to 41% (0.65 vol.% O_2)

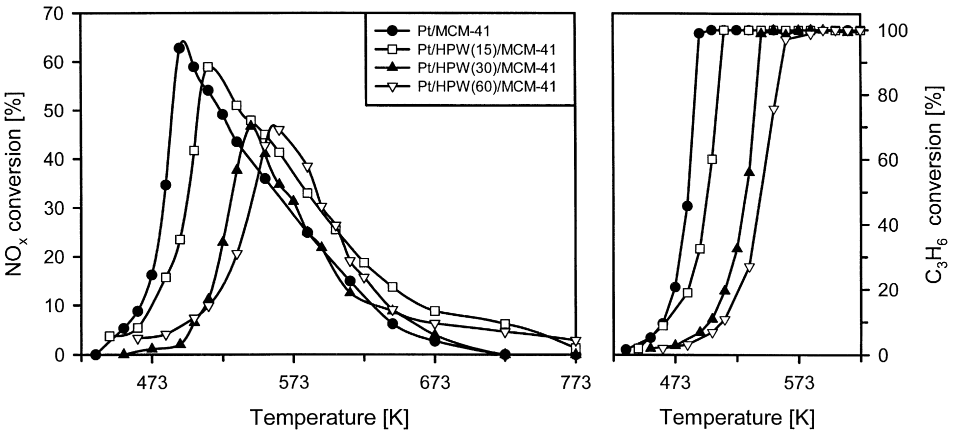

Fig. 1. Conversion of NO_x and C_3H_6 over Pt/HPW/MCM-41 as function of the temperature.

Table 2
NO_x conversion and N_2 selectivity of the Pt/HPW/MCM-41 catalysts

Sample	NO_x conversion (%)	Temperature at maximum conversion (K)	N_2 selectivity (%)
Pt/MCM-41	62	483	35
Pt/HPW(15)/MCM-41	60	493	35
Pt/HPW(30)/MCM-41	50	503	40
Pt/HPW(60)/MCM-41	47	513	45

and from 45 (10.0 vol.% O_2) up to 54% (0.68 vol.% O_2) on Pt/MCM-41 and on Pt/HPW(30)/MCM-41, respectively.

The effect of adding 2.5 vol.% water vapor into the gas stream on the NO_x conversion at 573 K is shown in Fig. 3. At this temperature, the NO_x conversion without water being present was around 30% over both catalysts. After stepwise adding 2.5 vol.% water vapor into the gas stream, the NO_x conversion over Pt/MCM-41 decreased to 28%, while over Pt/HPW(30)/MCM-41, it increased initially to 42% and reached a constant level of 39% within 1 h time on stream. After removal of the water vapor from the feed, the activity of Pt/MCM-41 immediately returned to the initial value (30%). On Pt/HPW(30)/MCM-41, the NO_x conversion reached a constant level of 36%, while the initial NO_x conversion level could only be restored on the Pt/HPW(30)/MCM-41 catalyst after heating to 773 K in He for 1 h.

The influence of the water vapor concentration on the activity at 573 K of the catalysts loaded with increasing concentrations of $H_3PW_{12}O_{40}$ is shown in Fig. 4. At this temperature, the activity and selectivity of the catalysts at reaction conditions without water vapor being present was independent of the $H_3PW_{12}O_{40}$ loading. On all tungstophosphoric acid containing catalysts, an increase in the NO_x conver-

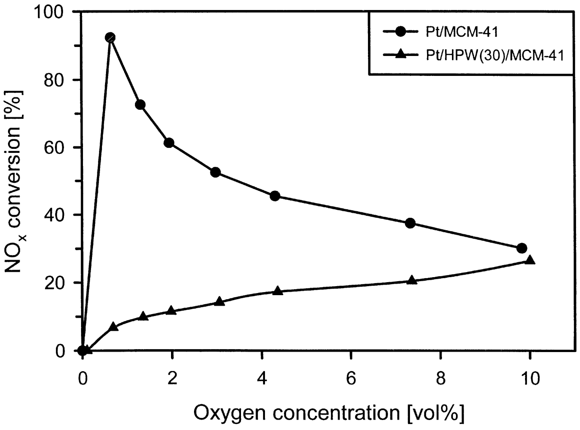

Fig. 2. Effect of oxygen concentration on the NO_x conversion at 513 K.

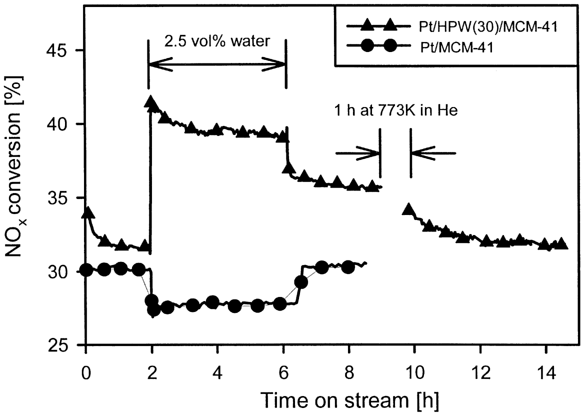

Fig. 3. Changes in activity in presence of water vapor at 573 K.

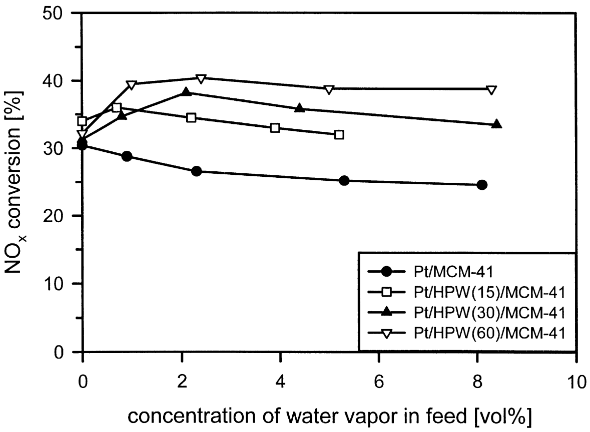

Fig. 4. Influence of water vapor concentration on the activity of Pt/HPW/MCM-41 at 573 K.

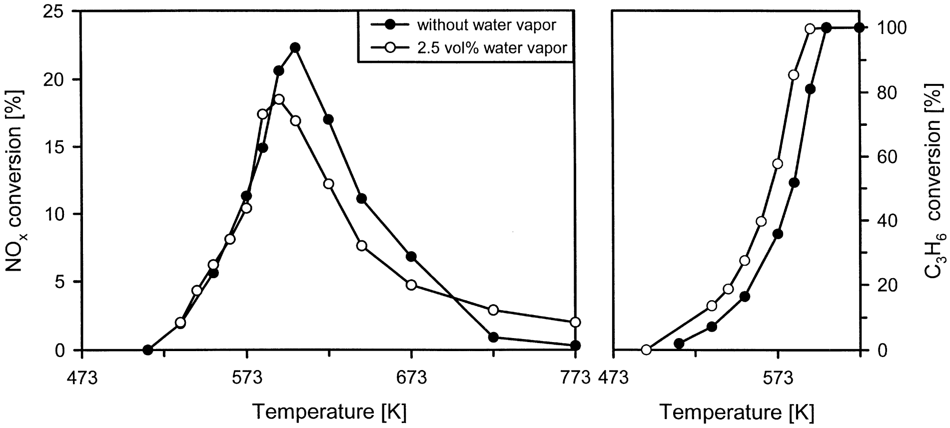

Fig. 5. NO_x and C_3H_6 conversion over HPW(30)/MCM-41 in the presence of 2.5 vol.% water vapor.

sion in the presence of water vapor was observed, while for Pt/MCM-41, the activity continuously decreased. On Pt/HPW(60)/MCM-41, the catalyst with the highest $H_3PW_{12}O_{40}$ loading, the NO_x conversion increased from 30 to 40% (i.e. a 25% higher relative conversion level compared to the water-free reaction conditions) at water vapor concentrations above 2 vol.%.

The effect of water vapor on the NO_x and C_3H_6 conversion of HPW(30)/MCM-41 is shown in Fig. 5. On the metal-free catalyst, the NO_x conversion started independently of the presence of water vapor at the same temperature and showed an identical trend until the maximum NO_x conversion was reached. In the absence of water vapor, the maximum NO_x conversion was 22% at 603 K, while in the presence of water vapor, the maximum NO_x conversion was 18.5% at 593 K. Also the C_3H_6 conversion was found to be significantly influenced by the presence of water vapor as the complete C_3H_6 conversion was reached at a temperature of 593 K compared to 603 K in the absence of water vapor.

The NO_x conversion as a function of the C_3H_6 concentration over Pt/HPW(30)/MCM-41 at 573 K with and without water vapor being present is shown in Fig. 6 (NO_x concentration 1010 ppm). Independent of the presence of water vapor, the NO_x conversion increased almost linearly up to a C_3H_6 concentration of 2100 ppm, a further increase in the concentration of the hydrocarbon did not result in a higher NO_x conversion. At C_3H_6 concentrations below 1550 ppm, the NO_x conversion was higher in the presence of water vapor, while above this concentration, the catalyst was more active under water-free reaction conditions. At the highest propene concentration, the NO_x conversion was 64% under water-free reaction conditions compared to 58% in the presence of water vapor.

The type and density of acid sites, generated by the impregnation of Pt/MCM-41 with $H_3PW_{12}O_{40}$, was studied by adsorption of pyridine (1×10^{-1} mbar) and water (9×10^{-1} mbar) at 423 K. The IR-spectra of Pt/HPW(30)/MCM-41 and of siliceous MCM-41 shown in Fig. 7 were normalized to the structural vibrations of MCM-41 between 2100 and 1770 cm^{-1},

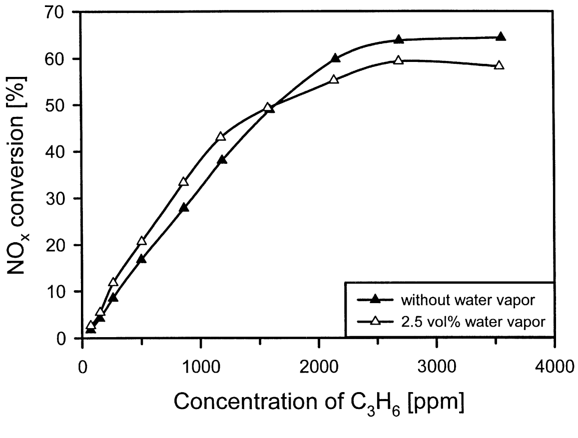

Fig. 6. NO_x conversion of Pt/HPW(30)/MCM-41 as function of C_3H_6 concentration (NO_x concentration 1010 ppm).

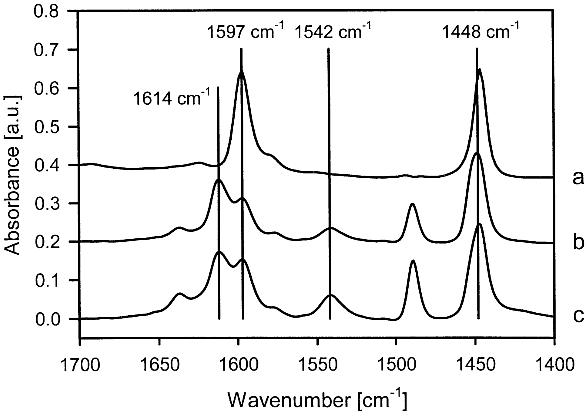

Fig. 7. Different IR-spectra at 423 K after adsorption of: (a) 10^{-1} mbar pyridine on siliceous MCM-41; (b) 10^{-1} mbar pyridine on Pt/HPW(30)/MCM-41 and (c) 10^{-1} mbar pyridine and 9×10^{-1} mbar H_2O on Pt/HPW(30)/MCM-41.

other experimental details are described in [23]. After adsorption of pyridine on siliceous MCM-41, only bands assigned to hydrogen-bonded pyridine (1449 and 1600 cm^{-1}) [24] were observed, while on Pt/HPW(30)/MCM-41, Brønsted type acid sites, indicated by the bands at 1540 and 1614 cm^{-1}, were additionally present. After the co-adsorption of 9×10^{-1} mbar H_2O on Pt/HPW(30)/MCM-41, the concentration of Brønsted type acid sites increased to about 75%, while the concentration of Lewis type acid sites was not affected by the presence of water vapor.

The number of accessible Pt atoms of the Pt/HPW/MCM-41 catalysts before and after reaction for 24 h at 573 K in the presence of 2.5 vol.% water vapor, determined by CO adsorption, is summarized in Table 3. While for Pt/MCM-41, the H/Pt ratio was not affected after the reaction, on catalysts loaded with $H_3PW_{12}O_{40}$, a significant reduction of the number of accessible metal atoms was observed.

Table 3
H/Pt ratio of the catalysts before and after reaction for 24 h at 2.5 vol.% water vapor

Sample	H/Pt ratio before reaction	H/Pt ratio after reaction
Pt/MCM-41	0.63	0.60
Pt/HPW(15)/MCM-41	0.16	0.09
Pt/HPW(30)/MCM-41	0.31	0.12
Pt/HPW(60)/MCM-41	0.10	0.06

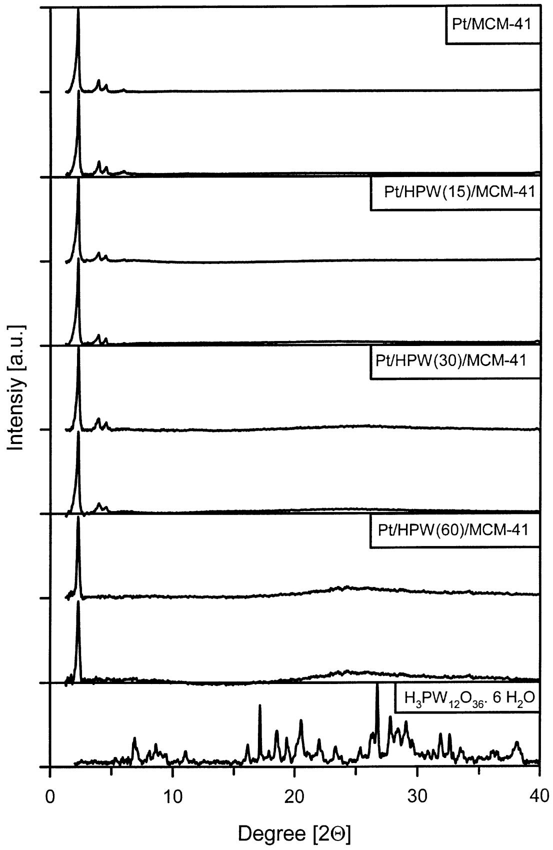

Fig. 8. Comparison of the XRD patterns before (top) and after reaction (bottom trace) for 24 h in the presence of 2.5 vol.% H_2O.

The XRD patterns of the catalysts before and after reaction at 573 K for 24 h in the presence of 2.5 vol.% water vapor are compared in Fig. 8. All catalysts showed the typical XRD pattern of MCM-41 type materials with a very strong (1 0 0) and additional (1 1 0), (2 0 0) and (2 1 0) reflexes [25]. From the position of the (1 0 0) reflex, a unit cell size of 39.4 Å was determined for the MCM-41 support. With increasing $H_3PW_{12}O_{40}$ loading of the catalysts, the intensity of the (1 1 0), (2 0 0) and (2 1 0) reflexes decreased. On Pt/HPW(60)/MCM-41, where only the (100) reflex could be observed, additionally a broad diffraction pattern in the region of $2\theta=15$–35° was present. However, even on Pt/HPW(60)/MCM-41, reflexes from crystalline $H_3PW_{12}O_{40}$ were not observed as shown by the comparison with the XRD pattern of $H_3PW_{12}O_{40}\cdot6H_2O$.

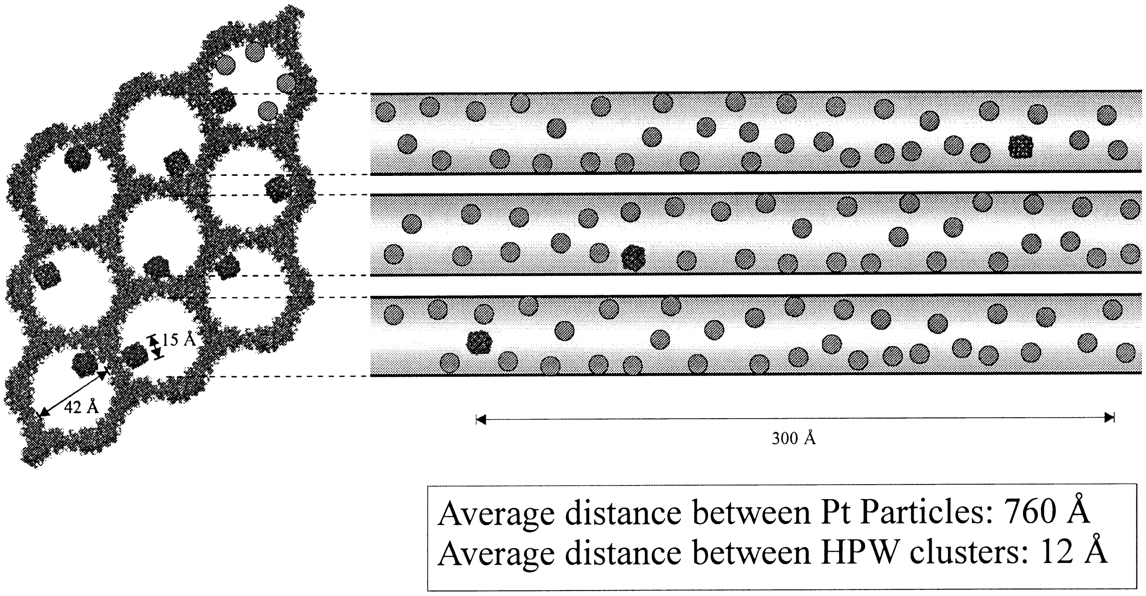

Fig. 9. Dimensions of the Pt and $H_3PW_{12}O_{40}$ clusters in MCM-41.

Fig. 9 shows a schematic representation of MCM-41 with a pore diameter of 42 Å containing 1.6 wt.% Pt and 60 wt.% $H_3PW_{12}O_{40}$. The size of the clusters was chosen according to EXAFS results for Pt [26] and to literature data for $H_3PW_{12}O_{40}$ [17].

4. Discussion

Loading of Pt/MCM-41 catalysts with $H_3PW_{12}O_{40}$ led to an increase in the selectivity to N_2 formation and to a decrease in the catalytic activity for the reduction of NO_x with propene. The strong decrease in the number of accessible Pt atoms indicated that the tungstophosphoric acid partially covers the metal atoms, which led to a lower activity of the catalyst. The main product of the NO_x reduction over Pt/MCM-41 was N_2O, which is characteristic for Pt group metals supported on oxides [27,28].

On the $H_3PW_{12}O_{40}$ containing catalysts, the NO_x conversion was significantly enhanced in the presence of water vapor [19], while on Pt/MCM-41, similar to most other catalysts reported [8–10], the presence of water vapor led to a lower NO_x conversion. It is important to note that after adding water vapor to the reactant gas mixture, the activity immediately changed on the Pt/MCM-41 catalysts, while on Pt/HPW(30)/MCM-41, an induction period of about 30 min was observed, where the final conversion level was slowly reached. A similar behavior was also observed after removing the water vapor from the gas stream, where a treatment of the catalyst in He at 773 K for 1 h was necessary to reach the initial conversion level (see Fig. 5). The presence of the induction period indicated that the structural properties of the $H_3PW_{12}O_{40}$ component are affected by the water vapor. In contrast, changes in the sorption properties such as, e.g. a preferred adsorption of one of the reactants in the presence of water vapor should result in an immediate change in activity as observed on Pt/MCM-41.

IR-spectra clearly revealed that in the absence of water vapor, only a small concentration of Brønsted type acid sites was present on the $H_3PW_{12}O_{40}$ containing catalysts. After the co-adsorption of water, the concentration of Brønsted type acid sites strongly increased (75%), while the concentration of Lewis type acid sites did not change. Also the number of accessible Pt atoms was affected by the loading with $H_3PW_{12}O_{40}$. It was reported that partially hydrated $H_3PW_{12}O_{40}$ supported on MCM-41 type materials forms Keggin type units with an approximate diameter of 12 Å [17]. As shown in Fig. 9, the pore diameter of the mesoporous MCM-41 type support is sufficiently large to allow a deposition of Pt and $H_3PW_{12}O_{40}$ clusters, even at a loading of 60 wt.%, without blocking the accessibility of both sites for the reactants. Also the absence of XRD reflexes from crystalline $H_3PW_{12}O_{40}{\cdot}6H_2O$ in the Pt/HPW/MCM-41 catalysts confirmed the formation of small clusters of tungstophosphoric acid inside the pores. Nevertheless, the number of accessible metal atoms strongly decreased on the $H_3PW_{12}O_{40}$ containing catalysts especially after 24 h reaction time, which indicated that the tungstophosphoric acid was partially deposited on the surface of the metal particles.

These experiments revealed that the metal and the tungstophosphoric acid are in an immediate contact, which seems to be essential to achieve the additional activity in the presence of water vapor. Note that the role of Pt in the catalytic reduction of NO_x in an oxidative atmosphere depends on the type of the reducing agent applied [29]. For reactions using unsaturated hydrocarbons as reducing agent (e.g. C_3H_6), it was described that the NO_x reduction occurs only on the Pt particles, that the metal particles are in a reduced state and that their surface is mainly covered with carbonaceous species under reaction conditions. In contrast, during reactions using saturated hydrocarbons as reducing agent (e.g. C_3H_8), the metal surface is mainly covered with oxygen and the reaction of NO_x and the hydrocarbon species occurs on the interface between the metal and the oxide support. Recently, McCormic and coworkers [30,31] reported that after adsorption of NO on hydrated tungstophosphoric acid supported on SiO_2, protonated species were formed (i.e. NOH^+), which were almost completely decomposed (70–100% NO conversion) into N_2 and N_2O ($\sim$50% selectivity to N_2) in the presence of O_2 and H_2O around 700 K. The authors described a combined adsorption/decomposition mechanism, where tungstophosphoric acid adsorbs NO into the bulk structure, i.e.

$$H_3PW_{12}O_{40} \cdot 6H_2O + 3NO \\ \rightarrow H_3PW_{12}O_{40} \cdot 3NO + 6H_2O$$

and subsequently a decomposition of NO into N_2 and O_2 was proposed. The reactions reported in this paper, however, were carried out at a much lower temperature (573 K), where the NO_x conversion over the HPW(30)/MCM-41 catalyst was only 8%. Supported tungstophosphoric acid, in general known to be a very active catalyst for oxidation reactions [32], led to an increase of the C_3H_6 conversion and to a decrease of the NO_x conversion in the presence of water vapor (see Fig. 5). Therefore, the activity increase in the presence of water observed on Pt/HPW/MCM-41 cannot be explained by a suppression of the direct oxidation of the hydrocarbon. Also the experiments indicated that an additive contribution of $H_3PW_{12}O_{40}$ to the activity of the metal component was not the main reaction route contributing to the increase in the overall activity observed in the presence of water vapor.

Therefore, we would like to speculate that the improved activity of Pt/HPW/MCM-41 in the presence of water vapor results from a reaction occurring at the interface between the metal and the acid sites. The conversion of NO_x observed as a function of the propene concentration indicated that the hydrocarbon was partially adsorbed on the tungstophosphoric acid. Thus, we would further like to speculate that C_xH_y species, formed by the adsorption of C_3H_6 on the Brønsted type acid sites, react with NO adsorbed on the metal sites. The formation of highly acidic Brønsted type acid sites on the hydrated tungstophosphoric acid (see Fig. 7) generated additional adsorption sites, which increased the local concentration of reducing agent on the perimeter between the acid and the metal clusters and thus gave rise to the higher activity in the presence of water vapor. With increasing C_3H_6/NO_x ratio, the local concentration of C_3H_6 approached a level where it started to displace NO from the metal sites and, therefore, the activity did not further increase. In the presence of water vapor, this effect was more pronounced, because the concentration of Brønsted type acid sites was higher. Consequently, Pt/HPW/MCM-41 catalysts were more active in the presence of water vapor at lower C_3H_6 concentrations. However, in the presence of water vapor, the critical concentration of reducing agent was reached at a lower C_3H_6/NO_x ratio and, therefore, the Pt/HPW/MCM-41 catalysts were more active when water vapor was not present at high concentrations of reducing agent.

5. Conclusions

The loading of Pt/MCM-41 with $H_3PW_{12}O_{40}$ improved the selectivity towards N_2 formation and the activity in the presence of water vapor, but led to a slightly lower activity of the catalysts in the catalytic reduction of NO_x with C_3H_6. Contrary to all other catalysts studied so far, Pt/HPW/MCM-41 catalysts showed a significant increase in the NO_x conversion in the presence of water vapor, while for Pt/MCM-41, a small suppression of the NO_x conversion was found.

The improved activity of the Pt/HPW/MCM-41 catalysts is attributed to the generation of Brønsted type acid sites on the hydrated $H_3PW_{12}O_{40}$, which act as additional sorption sites for the reducing agent. These sites, only present on hydrated $H_3PW_{12}O_{40}$, enhance the local concentration of C_3H_6 on the surface of $H_3PW_{12}O_{40}$ containing catalysts in the presence of water vapor. At high C_3H_6 concentrations, however, the concentration reached a level where the reducing agent displaces the NO from the metal sites, and consequently, the activity of $H_3PW_{12}O_{40}$ containing catalysts was lower for reactions at high C_3H_6/NO_x ratios compared to reactions in the absence of water vapor.

The advantages of using MCM-41 type materials as support result from the high specific surface area of these materials (in the order of $\sim$1000 m^2/g) and from the regular pore sizes compared to other oxide supports. This allows to achieve a high loading with metallic and acidic clusters without observing severe limitations in the accessibilities of these sites for the reactants.

Acknowledgements

The work was supported by the “Hochschuljubiläumsfonds der Österreichischen Nationalbank” under Project 7119.

References

[1] C.T. Bowmann, in: Proceedings of the 24th Symposium on Combustion, 1992, p. 859.
[2] J.N. Armor, Catal. Today 38 (1977) 163.
[3] H. Bosch, F. Janssen, Catal. Today 2 (1988) 369.
[4] J.N. Armor, Catal. Today 26 (1995) 99.
[5] M. Iwamoto, H. Furukawa, Y. Mine, F. Uemura, S. Mikuriya, S. Kagawa, J. Chem. Soc., Chem. Commun. (1986) 1271.
[6] Y. Li, J. Armor, Appl. Catal. B 1 (1992) L31.
[7] A.J. Desai, V.I. Kovalchuk, E.A. Lombardo, J.L. d’Itri, J. Catal. 184 (1999) 396.
[8] M. Iwamoto, N. Mizuno, H. Yahiro, in: Proceedings of the 10th International Congress on Catalysis, Budapest, 1992, p. 1285.
[9] H.Y. Chen, W.M.H. Sachtler, Catal. Lett. 50 (1998) 125.
[10] S. Sumiya, M. Saito, H. He, Q.C. Feng, N. Takezawa, K. Yoshida, Catal. Lett. 50 (1998) 87.
[11] X. Feng, W.K. Hall, J. Catal. 166 (1997) 368.
[12] R.W. Joyner, M. Stockenhuber, Catal. Lett. 45 (1997) 15.
[13] M. Iwamoto, H. Yahiro, H.K. Shin, M. Watanabe, J. Guo, M. Konno, T. Chikahisa, T. Murayama, Appl. Catal. B 5 (1994) L1.
[14] H. Hamada, Y. Kintaichi, M. Sasaki, Y. Ito, Appl. Catal. 75 (1991) L1.
[15] R. Burch, P.J. Millington, Catal. Today 26 (1995) 185.
[16] A. Jentys, N.H. Pham, H. Vinek, J. Chem. Soc., Faraday Trans. 92 (1996) 3287.
[17] I.V. Kozhevnikov, A. Sinnema, R.J.J. Jansen, K. Pamin, H. Van Bekkum, Catal. Lett. 30 (1995) 241.
[18] C.F. Cheng, D.H. Park, J. Klinowski, J. Chem. Soc., Faraday Trans. 93 (1997) 193.
[19] W. Schießer, H. Vinek, A. Jentys, Catal. Lett. 56 (1998) 189.
[20] A. Jentys, W. Schießer, H. Vinek, J. Chem. Soc., Chem. Commun. (1999) 335.
[21] W. Thompson, Philos. Mag. 42 (1871) 448.
[22] R. Schmidt, E.D. Hansen, M. Stöcker, D. Akporiaye, O.H. Ellestad, J. Am. Chem. Soc. 117 (1995) 4049.
[23] A. Jentys, N.H. Pham, H. Vinek, J. Chem. Soc., Faraday Trans. 92 (1996) 3287.
[24] J. Ward, J. Catal. 9 (1967) 225.
[25] F. Schüth, Ber. Bunsenges. Phys. Chem. 99 (1995) 1315.
[26] A. Jentys, W. Schießer, H. Vinek, Catal. Lett. 47 (1997) 193.
[27] M.D. Amiridis, T. Zhang, R.J. Farrauto, Appl. Catal. B 10 (1996) 203.
[28] N.W. Cant, D.E. Angove, D.C. Chambers, Appl. Catal. B 17 (1998) 63.
[29] R. Burch, J.A. Sullivan, T.C. Watling, Catal. Today 42 (1998) 13.
[30] A.M. Herring, R.L. McCormic, J. Phys. Chem. B 102 (1998) 3175.
[31] R.L. McCormic, S.K. Boonrueng, A.M. Herring, Catal. Today 42 (1998) 145.
[32] F. Cavani, Catal. Today 41 (1998) 73.